

University of Groningen

## Automatic differentiation of u- and n-serrated patterns in direct immunofluorescence images

Shi, Chenyu; Guo, Jiapan; Azzopardi, George; Meijer, Joost; Jonkman, Marcel F.; Petkov, Nicolai

*Published in:*  
Computer Analysis of Images and Patterns

**IMPORTANT NOTE:** You are advised to consult the publisher's version (publisher's PDF) if you wish to cite from it. Please check the document version below.

*Document Version*  
Publisher's PDF, also known as Version of record

*Publication date:*  
2015

[Link to publication in University of Groningen/UMCG research database](#)

### *Citation for published version (APA):*

Shi, C., Guo, J., Azzopardi, G., Meijer, J., Jonkman, M. F., & Petkov, N. (2015). Automatic differentiation of u- and n-serrated patterns in direct immunofluorescence images. In Computer Analysis of Images and Patterns (Vol. 9256, pp. 513-521). (Lecture Notes in Computer Science). Springer.

### **Copyright**

Other than for strictly personal use, it is not permitted to download or to forward/distribute the text or part of it without the consent of the author(s) and/or copyright holder(s), unless the work is under an open content license (like Creative Commons).

### **Take-down policy**

If you believe that this document breaches copyright please contact us providing details, and we will remove access to the work immediately and investigate your claim.

*Downloaded from the University of Groningen/UMCG research database (Pure): <http://www.rug.nl/research/portal>. For technical reasons the number of authors shown on this cover page is limited to 10 maximum.*

# Automatic differentiation of u- and n-serrated patterns in direct immunofluorescence images

Chenyu Shi<sup>1</sup>, Jiapan Guo<sup>1</sup>, George Azzopardi<sup>1,2</sup>,  
Joost M. Meijer<sup>3</sup>, Marcel F. Jonkman<sup>3</sup>, and Nicolai Petkov<sup>1</sup>

<sup>1</sup>Johann Bernoulli Institute for Mathematics and Computer Science,  
University of Groningen, Netherlands

<sup>2</sup> Intelligent Computer Systems, University of Malta, Malta

<sup>3</sup>Dermatology for Medical Sciences, University Medical Center Groningen (UMCG),  
University of Groningen, Netherlands  
`{c.shi,j.guo,g.azzopardi,n.petkov}@rug.nl`  
`{j.m.meijer01,m.f.jonkman}@umcg.nl`

**Abstract.** Epidermolysis bullosa acquisita (EBA) is a subepidermal autoimmune blistering disease of the skin. Manual u- and n-serrated patterns analysis in direct immunofluorescence (DIF) images is used in medical practice to differentiate EBA from other forms of pemphigoid. The manual analysis of serration patterns in DIF images is very challenging, mainly due to noise and lack of training of the immunofluorescence (IF) microscopists. There are no automatic techniques to distinguish these two types of serration patterns. We propose an algorithm for the automatic recognition of such a disease. We first locate a region where u- and n-serrated patterns are typically found. Then, we apply a bank of *B*-COSFIRE filters to the identified region of interest in the DIF image in order to detect ridge contours. This is followed by the construction of a normalized histogram of orientations. Finally, we classify an image by using the nearest neighbors algorithm that compares its normalized histogram of orientations with all the images in the dataset. The best results that we achieve on the UMCG publicly available data set is 84.6% correct classification, which is comparable to the results of medical experts.

**Keywords:** Serration patterns analysis, direct immunofluorescence image, COSFIRE filter, ridge detection, skin disease

## 1 Introduction

Epidermolysis bullosa acquisita (EBA) is a subepidermal autoimmune blistering disease of the skin which shares similar clinical features with other types of pemphigoid [14]. To differentiate EBA from these other types, serration pattern analysis in direct immunofluorescence (DIF) images is used by clinical experts [4, 10, 11, 13]. Such analysis concerns two types of serrated patterns, named u- and n-serrated patterns. Fig. 1(a-b) show examples of u-serrated and n-serrated pattern images. These two types of patterns are typically located along the

boundary between the green and dark regions, which are marked by red dashed lines in Fig. 1. We refer to this boundary as the region of interest. Fig. 1c shows an example of a u-serrated pattern, characteristic are the finger-like shapes pointing upwards. The presence of such a pattern is an indication for EBA. Fig. 1d shows an n-serrated pattern that contains undulating n-shapes. Such patterns are found in other types of pemphigoid. The manual analysis of serration patterns in DIF images is very challenging, mainly due to noise and lack of training of the immunofluorescence (IF) microscopists [6, 10]. So far there are no automatic techniques to distinguish between these two types of serration patterns.

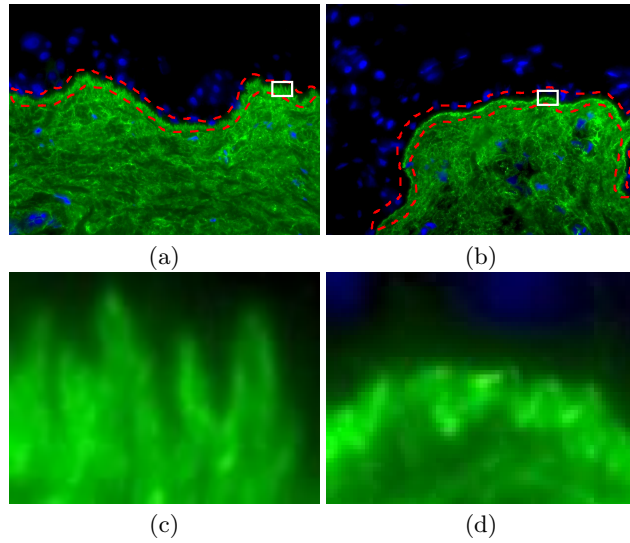


**Fig. 1.** Example of (a) a u-serrated and (b) an n-serrated pattern image. The areas marked by the red dashed lines indicate the regions of interest. (c-d) Enlargement of the enframed u- and n-serrated patterns in (a-b), respectively.

We propose an automatic method to recognize u- and n-serrated patterns. We apply a bank of *B*-COSFIRE filters [3], based on the existing COSFIRE approach [2], to the automatically identified regions of interest in DIF images in order to detect ridges and determine their orientations. Every image is then represented by a normalized histogram of orientations. We classify a test image by comparing its normalized histogram of orientations with those of the training images using a nearest neighbor approach.

The rest of the paper is organized as follows. In Section 2 we explain the proposed method. We report experiments in Section 3. Section 4 contains a discussion about certain aspects of the proposed method and we draw conclusions in Section 5.

## 2 Proposed method

### 2.1 Overview

Here we explain the main idea of the proposed method and subsequently we provide a detailed description of each step. First, we identify the region of interest in a DIF image, which is the wavy green boundary. For this region, we enhance the contrast and detect the ridges by applying *B*-COSFIRE filters [3] selective for six orientations (in intervals of 30 degrees). Finally, we compare the normalized histogram of orientations of a given test image to those of the training images and assign a label according to the nearest neighbors rule.

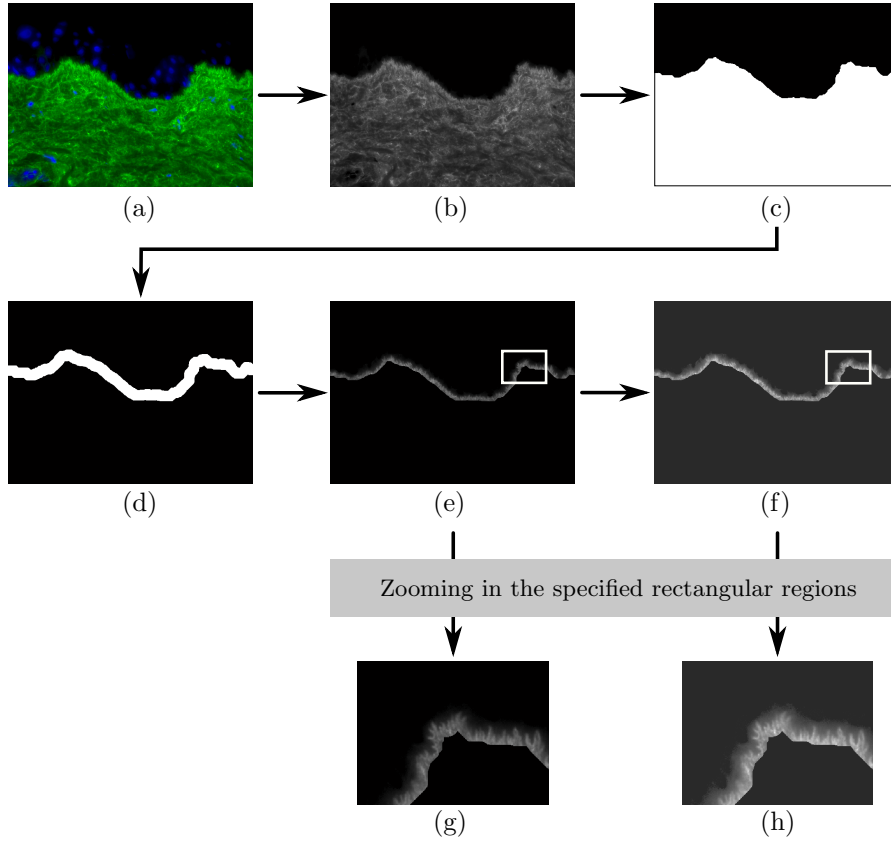


**Fig. 2.** Step-by-step illustration of the segmentation and enhancement of the region of interest. (a) Original RGB DIF image (of size  $1392 \times 1040$  pixels) and (b) its green channel. (c) Result of the application of a morphological closing by a disk-shaped structuring element (with radius of 30 pixels) to the green channel. (d) Result of broadening the boundary obtained in (c) by means of a morphological dilation by a disk-shaped structuring element (with radius of 30 pixels). (e) The product of the green channel image and the mask. (f) Contrast-limited adaptive histogram equalization (CLAHE) of the result image. (g-h) Enlargement of the respective enframed regions.

## 2.2 Segmentation of the region of interest

Fig. 2 illustrates the main steps of the segmentation and enhancement of the region of interest. Fig. 2a shows a RGB direct immunofluorescence image. We first perform morphological closing by a disk-shaped structuring element (radius of 30 pixels) to the green channel of the DIF image (Fig. 2b), the result of which is shown in Fig. 2c. If there are more than one connected components, we only consider the one with the largest area. Subsequently, we apply the Canny edge detector<sup>1</sup> [5] to delineate the region boundaries. As shown in Fig. 1 some images are characterized by one boundary between the green region and the background. Others are, however, characterized by two boundaries, Fig. 3. We only consider the upper-most<sup>2</sup> boundary in the image. Then, we obtain the region of interest by dilating the extracted boundary by a disk-shaped structuring element with a radius of 30 pixels, Fig. 2d. We use the resulting mask to extract the corresponding part of the green channel of the original image (Fig. 2e). Finally, we apply contrast-limited adaptive histogram equalization (CLAHE) to the segmented image (Fig. 2e) in order to improve the local contrast, Fig. 2f.

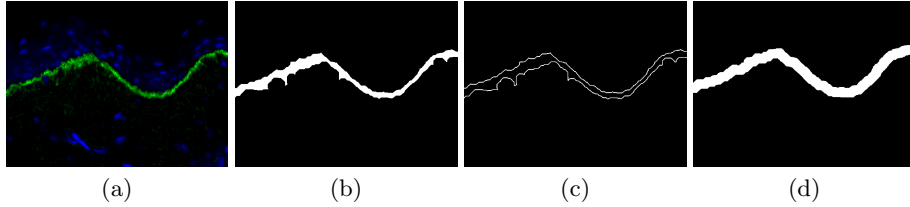


**Fig. 3.** (a) An example of a DIF image. (b) The largest connected component selected from the results of the morphological closing operation to the green channel of (a). (c) Two boundaries delineated by Canny edge detector from the image in (b). (d) The dilation result of the upper-most boundary.

## 2.3 *B*-COSFIRE filters

A *B*-COSFIRE filter<sup>3</sup> [3] is a ridge detector, which is based on the COSFIRE approach [2] and the CORF computational model [1]. Its response is achieved by computing the geometric mean of a group of linearly aligned responses of a Difference-of-Gaussians (DoG) filter.

We denote by  $r_{\sigma,l,\theta}(x,y)$  the response of a *B*-COSFIRE filter to a given input image at location  $(x,y)$ . Such a filter has three parameters: standard deviation  $\sigma$  of the outer Gaussian function in the involved DoG filter<sup>4</sup>, radius  $l$  and orientation  $\theta$ . The radius  $l$  is the farthest distance from the center of the filter

<sup>1</sup> We use the following parameters: standard deviation of  $\sqrt{2}$ , high threshold of 0.02 and low threshold of 0.01.

<sup>2</sup> We choose the upper-most boundary by comparing the mean of the y-coordinates of the two boundaries

<sup>3</sup> Matlab scripts: <http://www.mathworks.com/matlabcentral/fileexchange/49172>

<sup>4</sup> The standard deviation of the inner Gaussian function is  $0.5\sigma$

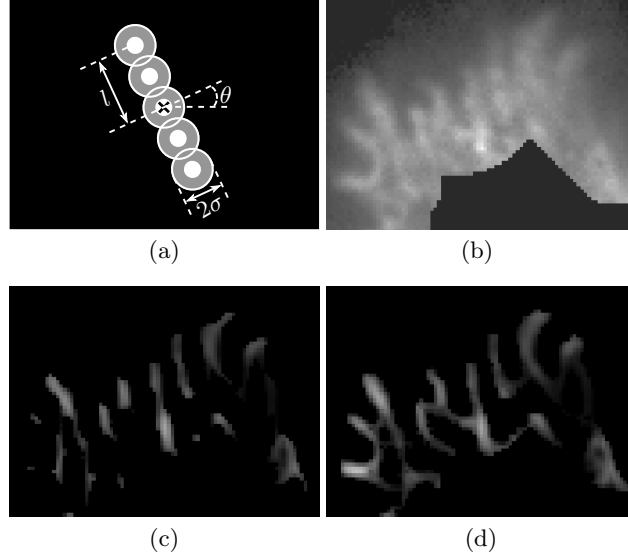


**Fig. 4.** (a) Structure of a  $B$ -COSFIRE filter selective for vertical ridges (orientation preference  $\theta = 30$ ). Its area of support has a radius  $l$  of 4 pixels and it takes as input five responses from a center-on DoG filter with  $\sigma = 1.2$ . For illustration clarity the diameter of the outer Gaussian functions here is  $2\sigma$  pixels. The afferent inputs are equally spaced in intervals of 2 pixels. The cross marker indicates the central position of the filter support and the concentric circles represent the area of support of the DoG function at the considered locations. (b) An input image and (c) the corresponding  $B$ -COSFIRE response map. (d) Superposition of the responses of a bank of  $B$ -COSFIRE filters selective for six different orientations:  $\theta \in \{0, \pi/6, \dots, 5\pi/6\}$ .

at which DoG responses are considered as input to a  $B$ -COSFIRE filter in a specific position, Fig. 4a. The original  $B$ -COSFIRE filters use a blurring function to allow for some tolerance with respect to the preferred position of DoG responses. Given the small size of the ridges in DIF images it was not necessary to blur<sup>5</sup> the DoG responses for this application. The responses of a  $B$ -COSFIRE filter are thresholded at a given fraction  $t$  ( $0 \leq t \leq 1$ ) of the maximum response of  $r_{\sigma,l,\theta}(x,y)$  across all the combinations of values  $(\sigma, l, \theta)$  and all the positions  $(x, y)$  in the image. For this application, we use a fixed threshold of 0.001. We comment on the choice of the values of  $\sigma$  and  $l$  in Sections 3 and 4. For further technical details we refer to [1–3, 7–9] and to an online implementation<sup>6</sup>.

Fig. 4a shows the structure of a  $B$ -COSFIRE filter with a standard deviation  $\sigma = 1.2$ , radius  $l = 4$  and orientation  $\theta = 30$ . The cross marker indicates the center of the area of support of the  $B$ -COSFIRE filter. As an illustration we apply this filter to the input image shown in Fig. 4b, which is cropped from Fig. 2f. The thresholded filter response map is shown in Fig. 4c. Fig. 4d shows the

<sup>5</sup> We set  $\sigma_0 = 0$  and  $\alpha = 0$  in the  $B$ -COSFIRE implementation.

<sup>6</sup> <http://matlabserver.cs.rug.nl>

superposition of thresholded responses of a bank of  $B$ -COSFIRE filters selective for six different orientations.

## 2.4 Histogram of orientations

Here, we explain how we form a feature vector from the responses of a bank of  $B$ -COSFIRE filters.

For each segmented and enhanced DIF image, we apply a bank of  $B$ -COSFIRE filters that are selective for six orientations:  $\theta \in (0, \pi/6, \dots, 5\pi/6)$ . This results in six response maps. Next, we create an orientation map by taking at each location the orientation of the  $B$ -COSFIRE filter that exhibits the maximum response. Finally, we construct the L1-normalized histogram of the resulting orientation map within the segmented region and use it as the feature vector of a given DIF image. Fig. 5(a-c) and Fig. 5(d-f) show normalized histograms of the orientation maps of three u-serrated patterns and three n-serrated patterns, respectively. It is interesting to observe that the u-serrated patterns result in valley-like shape histograms and the n-serrated patterns in a hill-like shape histograms.

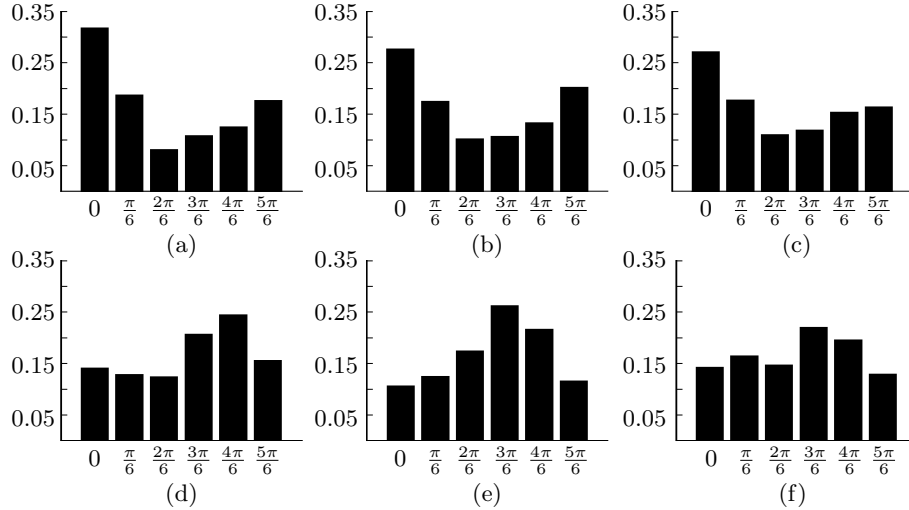


**Fig. 5.** Normalized histograms of orientation maps of (a-c) the three u-serrated patterns and (d-f) the three n-serrated patterns in Fig. 6, respectively.

## 3 Evaluation

### 3.1 Data set

We use a data set from an image-based online test [12] provided by the University Medical Center Groningen (UMCG). It comprises 26 DIF images from

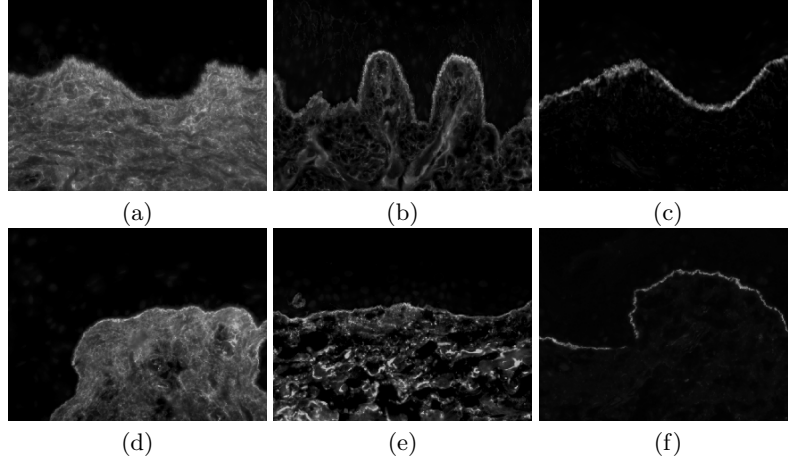


**Fig. 6.** The green channels of (a-c) three u-serrated and (d-f) three n-serrated patterns.

different pemphigoid patients, 11 of which contain u-serrated patterns and the rest contain n-serrated patterns. All images are taken with magnifications of  $\times 40$  and  $\times 63$ . We only consider the ones with  $\times 40$  magnification as they are the most commonly used in hospitals. Fig. 6(a-f) show six examples of gray scale DIF images which are described by the histograms in Fig. 5(a-f).

### 3.2 Experiments

We apply the methods proposed in Section 2 to the 26 DIF images and compute for every DIF image a normalized histogram of orientations. For the evaluation of the proposed method, we use the nearest neighbor algorithm to classify each image as u-serration or n-serration pattern by comparing its normalized histogram of orientations with the ones of the remaining 25 DIF images in the dataset. Considering that a *B*-COSFIRE filter uses parameters  $\sigma$  and  $l$ , we run various experiments by systematically changing the values of the parameters  $\sigma$  ( $\sigma \in \{0.5, 1, \dots, 5\}$ ) and  $l$  ( $l \in \{2, 4, 6\}$ ). Fig. 7 shows the experimental results with the highest correct classification rate being 84.6% (22 out of 26), which we achieve by using leave-one-out cross-validation. We achieve this result with two pairs of parameters,  $\sigma = 1.5$ ,  $l = 2$  and  $\sigma = 2.5$ ,  $l = 4$ , which are indicated by the large star and circle markers in Fig. 7, respectively.

## 4 Discussion

The classification rate of 84.6% which we achieve is comparable to the results obtained by trained medical experts in an online test [10]. In that test, there were three categories of experts with a priori knowledge on the subject; namely dermatology residents at the UMCG, dermatologists and pathologists who had



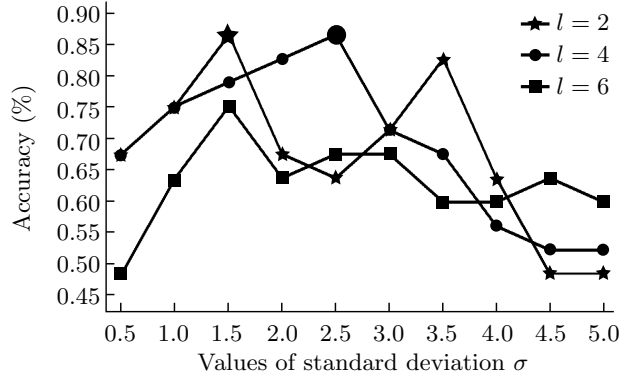


**Fig. 7.** Results achieved on the UMCG data set with different values of  $\sigma \in \{0.5, 1, \dots, 5\}$  and  $l \in \{2, 4, 6\}$  of the involved  $B$ -COSFIRE filters. The large star and circle indicate the highest classification rate we achieve.

participated in the annual Dutch blistering course in Groningen during 2005-2012, and international experts in blistering diseases. They were first asked to diagnose 13 DIF images. Then, they were given more information on the subject by means of an online instruction video<sup>7</sup> about n- and u-serrated patterns, and finally they were asked to diagnose the remaining 13 images. The performance achieved by these three groups of participants improved with training [10]. UMCG experts reached a performance of 82.1%, the participants from the blistering course achieved 72.8% and the international experts achieved 83.4%. The average recognition rate for all participants was 78.6%.

In future work, we aim to develop an algorithm that localizes the n- and u-serrated patterns in a DIF image, which is also useful to aide the medical experts in the diagnosis.

## 5 Conclusions

We propose an approach for the automatic classification of u- and n-serrated patterns in DIF images to distinguish EBA from other forms of pemphigoid. It is the first one that addresses the challenging problem of detecting EBA in DIF images. The algorithm that we propose can be considered as a computer aided diagnosis tool that may assist experts in the decision making process. We achieve a recognition rate of 84.6% on the UMCG public data set of 26 images, which is comparable to the performance of medical experts.

**Acknowledgment** We wish to thanks to the photographer and data manager of the dermatology department of UMCG for their valuable help.

<sup>7</sup> Online training: <http://www.nversusu.umcg.nl>

## References

1. Azzopardi, G., Petkov, N.: A CORF computational model of a simple cell that relies on LGN input outperforms the Gabor function model. *Biological Cybernetics* 106(3), 177–189 (2012)
2. Azzopardi, G., Petkov, N.: Trainable COSFIRE Filters for Keypoint Detection and Pattern Recognition. *IEEE Transactions on Pattern Analysis and Machine Intelligence* 35(2), 490–503 (Feb 2013)
3. Azzopardi, G., Strisciuglio, N., Vento, M., Petkov, N.: Trainable COSFIRE filters for vessel delineation with application to retinal images. *Medical Image Analysis* 19(1), 46–57 (JAN 2015)
4. Buijsrogge, J.J.A., Diercks, G.F.H., Pas, H.H., Jonkman, M.F.: The many faces of epidermolysis bullosa acquisita after serration pattern analysis by direct immunofluorescence microscopy. *British Journal of Dermatology* 165(1), 92–98 (JUL 2011)
5. Canny, J.: A Computational Approach to Edge Detection. *IEEE Transactions on Pattern Analysis and Machine Intelligence* 8(6), 679–698 (Nov 1986)
6. Gammon, W., Kowalewski, C., Chorzelski, T., Kumar, V., Briggaman, R., Beutner, E.: Direct immunofluorescence studies of sodium chloride-separated skin in the differential diagnosis of bullous pemphigoid and epidermolysis bullosa acquisita. *Journal of the American Academy of Dermatology* 22(4), 664–670 (1990)
7. Petkov, N.: Biologically motivated computationally intensive approaches to image pattern-recognition. *Future Generation Computer Systems* 11(4-5), 451–465 (Aug 1995), 1994 Europe Conference on High Performance Computing and Networking (HPCN Europe 94), Munich, Germany, 1994
8. Petkov, N., Kruizinga, P.: Computational models of visual neurons specialised in the detection of periodic and aperiodic oriented visual stimuli: Bar and grating cells. *Biological Cybernetics* 76(2), 83–96 (Feb 1997)
9. Petkov, N., Westenberg, M.: Suppression of contour perception by band-limited noise and its relation to non-classical receptive field inhibition. *Biological Cybernetics* 88(10), 236246 (Mar 2003)
10. Terra, J.B., Meijer, J.M., Jonkman, M.F., Diercks, G.F.H.: The n- vs. u-serration is a learnable criterion to differentiate pemphigoid from epidermolysis bullosa acquisita in direct immunofluorescence serration pattern analysis. *British Journal of Dermatology* 169(1), 100–105 (JUL 2013)
11. Terra, J.B., Pas, H.H., Hertl, M., Dikkers, F.G., Kamminga, N., Jonkman, M.F.: Immunofluorescence serration pattern analysis as a diagnostic criterion in antilaminin-332 mucous membrane pemphigoid: immunopathological findings and clinical experience in 10 Dutch patients. *British Journal of Dermatology* 165(4), 815–822 (OCT 2011)
12. UMCg: UMCg online test. (2013), <http://www.nversusu.umcg.nl/>
13. Vodegel, R., Jonkman, M., Pas, H., De Jong, M.: U-serrated immunodeposition pattern differentiates type VII collagen targeting bullous diseases from other subepidermal bullous autoimmune diseases. *British Journal of Dermatology* 151(1), 112–118 (JUL 2004)
14. Woodley, D.T., Briggaman, R.A., O’Keefe, E.J., Inman, A.O., Queen, L.L., Gammon, W.R.: Identification of the skin basement-membrane autoantigen in epidermolysis bullosa acquisita. *New England Journal of Medicine* 310(16), 1007–1013 (1984)